The American Journal of Pathology, Vol. 185, No. 10, October 2015

ELSEVIER

The American Journal of
PATHOLOGY
ajp.amjpathol.org

CELL INJURY, REPAIR, AGING, AND APOPTOSIS

TMIGD1 Is a Novel Adhesion Molecule That Protects Epithelial Cells from Oxidative Cell Injury

Emad Arafa,* Philip A. Bondzie,* Kobra Rezazadeh,* Rosana D. Meyer,* Edward Hartsough,* Joel M. Henderson,* John H. Schwartz,† Vipul Chitalia,† and Nader Rahimi*‡

From the Department of Pathology, Boston University Medical Campus, the Renal Section,† Department of Medicine, Boston Medical Center, Boston University School of Medicine, and the Department of Ophthalmology,‡ School of Medicine, Boston University Medical Campus, Boston, Massachusetts*

Accepted for publication June 18, 2015.

Address correspondence to Nader Rahimi, Ph.D., Department of Pathology, Boston University Medical Campus, 670 Albany St., Boston, MA 02118. E-mail: nrahimi@bu.edu.

Oxidative damage to renal tubular epithelial cells is a fundamental pathogenic mechanism implicated in both acute kidney injury and chronic kidney diseases. Because epithelial cell survival influences the outcome of acute kidney injury and chronic kidney diseases, identifying its molecular regulators could provide new insight into pathobiology and possible new therapeutic strategies for these diseases. We have identified transmembrane and immunoglobulin domain-containing 1 (TMIGD1) as a novel adhesion molecule, which is highly conserved in humans and other species. TMIGD1 is expressed in renal tubular epithelial cells and promotes cell survival. The extracellular domain of TMIGD1 contains two putative immunoglobulin domains and mediates self-dimerization. Our data suggest that TMIGD1 regulates transepithelial electric resistance and permeability of renal epithelial cells. TMIGD1 controls cell migration, cell morphology, and protects renal epithelial cells from oxidative- and nutrient-deprivation–induced cell injury. Hydrogen peroxide-induced oxidative cell injury downregulates TMIGD1 expression and targets it for ubiquitination. Moreover, TMIGD1 expression is significantly affected in both acute kidney injury and in deoxy-corticosterone acetate and sodium chloride (deoxy-corticosterone acetate salt)-induced chronic hypertensive kidney disease mouse models. Taken together, we have identified TMIGD1 as a novel cell adhesion molecule expressed in kidney epithelial cells that protects kidney epithelial cells from oxidative cell injury to promote cell survival. *(Am J Pathol 2015, 185: 2757–2767; http://dx.doi.org/10.1016/j.ajpath.2015.06.006)*

Kidney failure occurs when the kidneys lose their ability to function because of acute or chronic diseases.[1] Both acute kidney injury (AKI) and chronic kidney disease (CKD) are major kidney diseases associated with high rates of morbidity and mortality.[2] Although two distinct entities, emerging evidence strongly indicates close interconnection between AKI and CKD, wherein the occurrence of one strongly predicts the risk of the other.[3,4] This interconnection also points to the presence of possible common underlying molecular mechanisms in AKI and CKD.[4] Renal tubular epithelial cells constitute most of the renal mass and are the common damaged cell type in both AKI and CKD.[5,6] Hypoxia, ischemia reperfusion (IR) injury, and oxidative stress damage are common pathologic assaults that inflict injury on epithelial cells, and the endurance of these cells strongly influences the clinical outcome.[7,8]

Cell adhesion plays a major role in kidney injury and repair. In response to insults such as ischemia or toxins, kidney epithelial cells lose their cell–cell and cell–matrix interactions, leading to loss of cell polarity, increased permeability, and cell death.[9–11] These events contribute to intraluminal aggregation of cells and proteins, causing tubular obstruction.[12,13] The loss of cell adhesion in injured cells proceeds changes in the distribution of actin and actin-binding proteins with altered structural characteristics and cytoskeletal changes[10] that lead to reduced sodium transport and other impairments.[14] Kidney epithelium has a remarkable regenerative capacity after ischemic/toxic injury.

Supported in part by the NIH grants R21CA191970 and RO1EY017955 (N.R.) and grant RO1CA175382 (V.C.).

Disclosures: None declared.

E.A. and P.A.B. contributed equally to this work.

http://dx.doi.org/10.1016/j.ajpath.2015.06.006

During the repair process, kidney tubular epithelial cells undergo a complex series of regenerative events such as proliferation, migration, and epithelial−mesenchymal transition, leading to restoration of functional tubular epithelial cells.[15] Cell adhesion plays a prominent role in these regenerative processes.[16]

Recently, we identified immunoglobulin (Ig) and proline-rich receptor-1 (IGPR-1) as a novel cell adhesion molecule encoded by transmembrane and Ig domain-containing 2 (*TMIGD2*).[17] IGPR-1/TMIGD2 is expressed in human endothelial and epithelial cells but is absent in the mouse genome. IGPR-1 is involved in angiogenesis, and its activity regulates endothelial capillary tube formation and cell migration.[17] Our further investigation resulted in the identification of TMIGD1, the second family member of IGPR-1. TMIGD1 is predicted to be expressed in humans, mice, and other species. A recent study suggests that TMIGD1 is expressed in normal human colon epithelial cells, and its expression appears to be down-regulated in human colon tumors.[18] The data presented here suggest that TMIGD1 is expressed in kidney tubular epithelial cells and that it acts to protect kidney epithelial cells from oxidative cell injury. TMIGD1 expression changes in mouse AKI and in deoxycorticosterone acetate (DOCA) and sodium chloride (DOCA salt)-induced chronic hypertensive kidney disease models, suggesting a possible role for TMIGD1 in kidney cell injury.

Materials and Methods

Plasmids, shRNA, and Antibodies

A mouse TMIGD1 clone (cDNA clone MGC:74197, IMAGE:30311543) was purchased from Open Biosystems (Huntsville, AL) and subsequently was cloned as a *Myc* (alias c-*myc*) tag in its C-terminus into retroviral pQCXIP vector via NotI and BamH1 sites. *Myc*-tagged TMIGD1 was further sequenced to confirm its sequence identity. Rabbit polyclonal anti-TMIGD1 antibody was made against a peptide that corresponded to 20 amino acids in the extracellular domain of TMIGD1. TMIGD1 shRNA (catalog SC 94146-sh) was purchased from Santa Cruz Biotechnology (Dallas, TX). It consists of a pool of three to five lentiviral vector plasmids, each encoding TMIGD1-specific 19 to 25 nt (plus hairpin) shRNAs.

Cell Lines

Human embryonic kidney epithelial HEK-293 cells and human kidney tubular epithelial HK2 cells were grown in Dulbecco's Modified Eagle's Medium (DMEM), supplemented with 10% fetal bovine serum plus antibiotics. HEK-293 cells were used to express the TMIGD1 construct. The pMSCV-puro retroviral vector was used to clone Myc-tagged TMIGD1. Viruses were produced in 293-GPG cells as described.[19]

Cell Viability and Apoptosis Assays

The MTT assay, which is based on the reduction of tetrazolium salt by live cells, was used to measure cell survival as described.[20] In brief, cells (5×10^4 per well) were seeded in 24-well plates (quadruple wells per group). After overnight incubation, cells were washed with phosphate-buffered saline (PBS), replaced with serum-free medium, or other conditions as indicated in the figure legends, and subjected to MTT assay. Results were processed as recommended by the manufacturer. For fluorescence-activated cell sorting analysis, cells were grown in 60-cm plates, treated with hydrogen peroxide as indicated later, subjected to staining with Annexin V-fluorescein isothiocyanate Apoptosis Kit (BD Biosciences, San Jose, CA) according to the manufacturer's instructions, and analyzed by fluorescence-activated cell sorting flow cytometery.

Cell Permeability and TEER Assays

Cell permeability was performed as described.[21] Briefly, HEK-293 cells that expressed TMIGD1 or HK2 cells that expressed TMIGD1-shRNA cells and corresponding control cells were seeded on tissue culture polycarbonate membrane filters coated with collagen I (pore size, 3.0 μm) in 24-well Transwell plates at a seeding density of 200,000 cells/well. The complete DMEM was added to both the donor and the acceptor compartment and incubated at 37°C in a carbon dioxide incubator for at least 5 days or until a monolayer of cells was formed. Fluorescein isothiocyanate-dextran (70 KD, 100 μL of 1×) was added to each insert and incubated at 37°C in a carbon dioxide incubator for the indicated time. At the end of each time point, the inserts were removed, and solutions from the lower chambers were transferred into a 96-well plate and read at 485-nm excitation, 520-nm emission. For the transepithelial electrical resistance (TEER) assay, cells were similarly prepared, and TEER assay was performed with a Millicell ERS meter (Millipore, Bedford, MA). The values of TEER were determined by measuring the potential difference between the two sides of the cell monolayer as recommended by the manufacturer.

Cell Surface Biotinylation Assay

HEK-293 cells that expressed TMIGD1 were subjected to biotinylation assay with the use of a cell surface protein isolation kit (catalog 89881; Pierce Biotechnology, Rockford, IL), and biotinylated proteins were purified as recommended by the manufacturer. Briefly, cells were incubated with Sulfo-NHS-SS-Biotin [sulfosuccinimidyl-2-(biotinamido)ethyl-1, 3-dithiopropionate] for 30 minutes on ice. Cells were lyzed, and biotinylated proteins were purified by NeutrAvidin Agarose beads. The eluted biotinylated proteins were blotted for TMIGD1.

Cell Aggregation Assay

The assay was performed as previously described.[17] Briefly, cells were detached from the plates with 1 mmol/L EDTA in PBS solution, washed twice in 10% DMEM, and were

re-suspended in DMEM. Approximately 5×10^5 cells per 2.5 mL were incubated in a six-well plate precoated with 1% bovine serum albumin with gentle shaking at 37°C for 1 hour, followed by no shaking for 30 minutes. Cells were viewed under a light microscope, and images were taken.

Real-Time PCR

Total RNA was isolated with TRIzol reagent (Life Technologies, Carlsbad, CA). One microgram of total RNA from at least three mice per group was reverse transcribed with the High Capacity cDNA Reverse Transcription Kit (Life Technologies) according to the manufacturer's protocol. Gene expression was determined by quantitative PCR with the use of the RT^2 SYBR Green qPCR Mastermix kit according to the manufacturer's protocol. Specific PCR primers for mouse TMIGD1 (5′-GACCCGAATTCAGAAACAC-3′ and 5′-GCCCTTCTCAAAACGTA-3′; forward and reverse primers, respectively) were used to amplify TMIGD1. Mouse 18S PCR forward primer 5′-CGCCGCTAGAGGTGAAATTC-3′ and reverse primer 5′-GGTATTTGCTACGGCTGACC-3′ were used for amplification of 18S ribosomal RNA. Data are presented as fold increase of TMIGD1 normalized to the housekeeping gene, *18S*.

In Vitro GST Pull-Down Assay

The extracellular domain of TMIGD1 that encompassed the Ig domains was cloned into pGX2T vector, and recombinant protein was prepared as described.[22] The purified glutathione *S*-transferase (GST)-fusion TMIGD1 protein subsequently was used for GST pull-down assay. The assay was performed as described.[23] Briefly, HEK-293 cells that expressed TMIGD1 were grown in 10-cm plates. The plates were washed with H/S buffer (25 mmol/L HEPES, pH 7.4, 150 mmol/L NaCl, 2 mmol/L Na_3VO) and lyzed in EB lysis buffer (10 mmol/L Tris-HCl, 10% glycerol, pH 7.4, 5 mmol/L EDTA, 50 mmol/L NaCl, 50 mmol/L NaF, 1% Triton X-100, 1 mmol/L phenylmethylsulfonyl fluoride, 2 mmol/L Na_3VO_4, and 20 mg/mL aprotinin). The normalized cell lysates were incubated with equal amounts of immobilized GST fusion TMIGD1 or GST control for 3 hours at 4°C. The beads were washed with PBS solution with protease inhibitors. The eluted proteins were boiled in sample buffer and analyzed by Western blot analysis with the use of the appropriate antibody.

Bioinformatics Analysis

The online Ensembl Genome Browser (*http://www.ensembl.org*, last accessed May 18, 2015) was used to obtain genomic information of TMIGD1 such as determining chromosomal location, coding exons, etc. The online SUPERFAMILY annotation program (*http://supfam.cs.bris.ac.uk/SUPERFAMILY*, last accessed May 18, 2015) was used to generate phylogenetic tree and other structural/domain information. The online Swiss model 3D modeling program (*http://swissmodel.expasy.org/interactive*, last accessed May 18, 2015; registration required) was used to predict three-dimensional structure of TMIGD1.

Immunoprecipitation and Western Blot Analysis

Cells were prepared and lyzed as described.[24] Briefly, cells were washed twice with H/S buffer [25 mmol/L HEPES (pH 7.4), 150 mmol/L NaCl, and 2 mmol/L Na_3VO_4] and lyzed in lysis buffer that contained Triton X-100. The normalized cell lysates were immunoprecipitated as indicated in the figure legends, and immunoprecipitated proteins were subsequently subjected to Western blot analysis with the use of the appropriate antibody as indicated in the figure legends. Cell surface biotinylation was performed as described[17] and according to the recommendations of the manufacturer.

Cell Traction Assay

Cell traction assay was performed as previously described.[25] In brief, thin polyacrylamide gels (7.5% acrylamide and 0.2% bis-acrylamide) that contained 0.5-μm diameter red fluorescent latex spheres (FluoSpheres; Invitrogen, Carlsbad, CA) at 0.001% concentration were polymerized between a glutaraldehyde-treated 22-mm square coverslip and an untreated 12-mm round coverslip after adding tetramethylethylenediamine. The round coverslips were gently removed after 30 minutes of polymerization, and the substrate surface was chemically activated by immersing the substrate in pure hydrazine hydrate (Sigma-Aldrich, St. Louis, MO). Activated substrate assemblies were washed with 5% acetic acid and water for 1 hour each, immersed in poly-D-lysine (BD Biosciences), and washed extensively with PBS. Poly-D-lysine–coated substrates were plated with cells and incubated at 37°C in 5% CO_2, to allow cell attachment and spreading. Immediately before imaging, the cell-seeded substrate assemblies were mounted individually in 6-cm cell culture plates under standard media.

Traction force microscopy was performed with an automated upright epifluorescence microscope (Labophot 2; Nikon, Melville, NY) equipped with immersion objectives and an environmental chamber. Dell Optiplex GX280 computer running Simple PCI software version 6.1 (Hamamatsu Corporation, Sewickley, PA) was used to collect the required digital images. The substrate surface was initially scanned at low power with the use of bright field illumination to identify and record x,y coordinate locations of fields that contained candidate cells. Fourier transform traction cytometry was performed to extract substrate displacement and traction fields, and root mean square traction was generated by each cell, using software kindly provided by Dr. Donald E. Ingber (Wyss Institute for Biologically Inspired Engineering, Cambridge, MA) to J.M.H.[25]

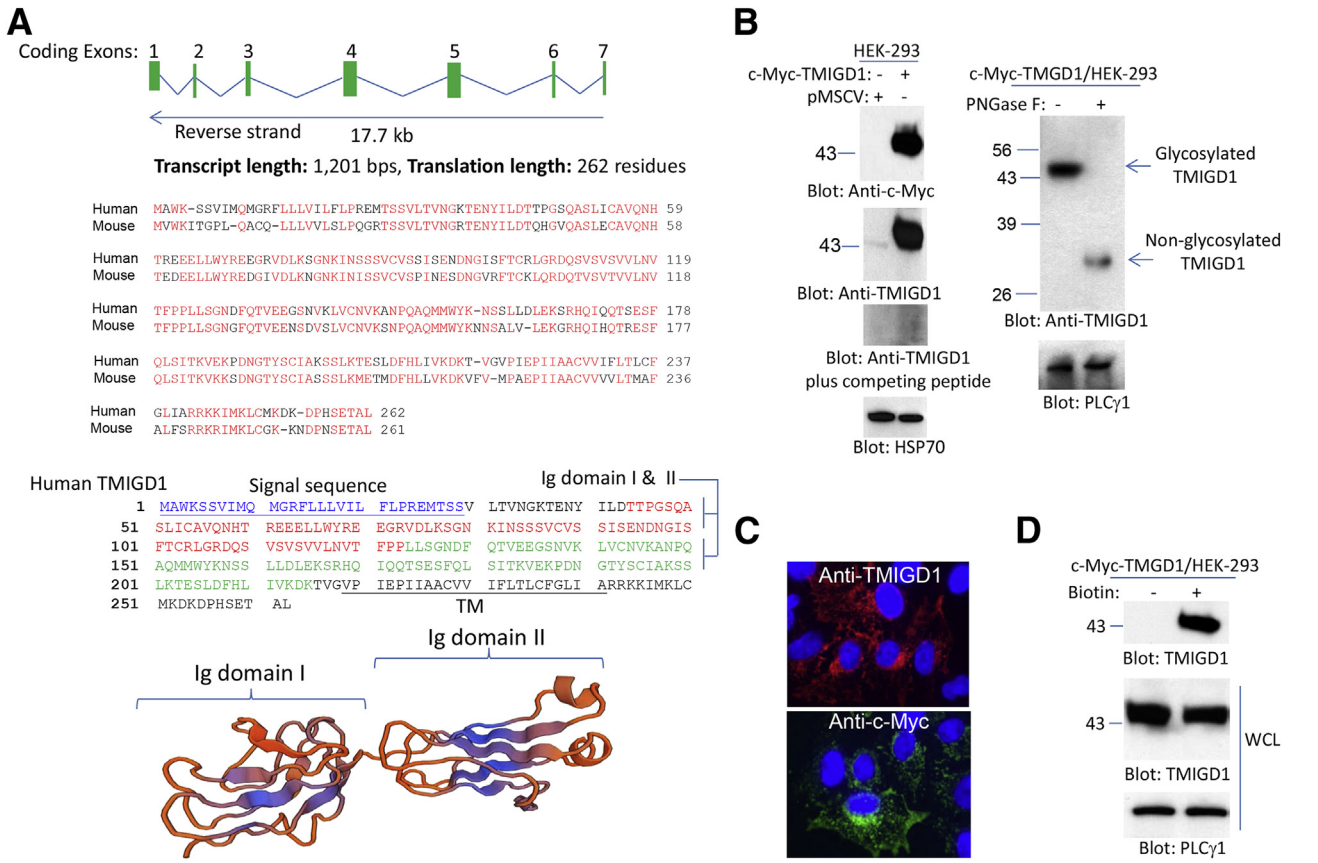

Figure 1 Identification and characterization of TMIGD1. **A:** Predicted human TMIGD1 mRNA and exons. Exons are not drawn to scale. Shown are the alignment of human TMIGD1 with mouse TMIGD1, amino acid sequences, and the predicted structure of Ig domain of TMIGD1. The signal sequence and TM domain of TMIGD1 are underlined. **B:** WCLs from HEK-293 cells that expressed pMSCV or *Myc*-tag-TMIGD1 were blotted with anti-*Myc* antibody or anti-TMIGD1 antibody. Preincubation of anti-TMIGD1 antibody with the TMIGD1 peptide blocks the recognition of TMIGD1. WCL was treated with the vehicle or PNGase F and blotted with anti-TMIGD1 antibody. The WCLs were also blotted for PLCγ1 for loading control. **C:** Immunofluorescence microscopy of HEK-293 cells that expressed TMIGD-1 with the use of anti-*Myc* or anti-TMIGD1 antibodies. **D:** HEK-293 cells that expressed *Myc*-TMIGD1 was subjected to cell surface biotinylation as described in *Materials and Methods* and blotted for TMIGD1. Aliquots of WCLs from the same group before purification with NeutrAvidin Agarose beads were blotted for TMIGD1 and loading control. Ig, immunoglobulin; pMSCV, empty retroviral vector; PLCγ1, phospholipase C- γ1; PNGase F, *N*-glycosidase F; TM, transmembrane; TMIGD1, transmembrane and immunoglobulin-containing 1; WCL, whole cell lysate.

Animal Models

DOCA Salt Uninephrectomy Model

Ten- to twelve-week-old 129/SVE mice were obtained from Taconic Farms (Germantown, NY). After a week of acclimatizing, surgeries were performed on mice. Mice were anesthetized by isoflurane inhalation and right uninephrectomy was performed, followed by implantation of a 21-day release DOCA salt pellet (Innovative Research of America, Sarasota, FL). After recovery from anesthesia, animals were housed singly in cages and fed on standard chow and given 1% saline as source of drinking water. Control animals were maintained on standard chow and tap water. For immunohistochemistry studies, mice were sacrificed at 0, 24 hours, and 2 weeks after DOCA salt uninephrectomy treatment.

Kidney IR Mouse Model

Six-week-old mice that weighed 20 to 22 g were used in the IR studies. After anesthesia with isoflurane, kidneys were exposed by generating a midline laparotomy. The left kidney was removed. Transient kidney ischemia was performed by clamping the right renal pedicles with the use of a nontraumatic vascular clamp for 25 minutes, an insult that produces severe, reversible acute renal failure.[26] The clamp was then removed, and restoration of blood flow (reperfusion) was visually confirmed. The abdominal section was closed with sutures. For histologic and immunohistochemistry analyses, mice were sacrificed 48 hours and 4 days after IR. Left kidneys served as control kidneys. Use of mice was approved by the Institutional Animal Care and Use Committee of Boston University.

Immunohistochemistry Analysis

Immunohistochemistry staining was performed as per the manufacturer's instruction with the use of the EXPOSE rabbit-specific horseradish peroxidase/diaminobenzidine detection immunohistochemical kit (Abcam, Cambridge, MA).

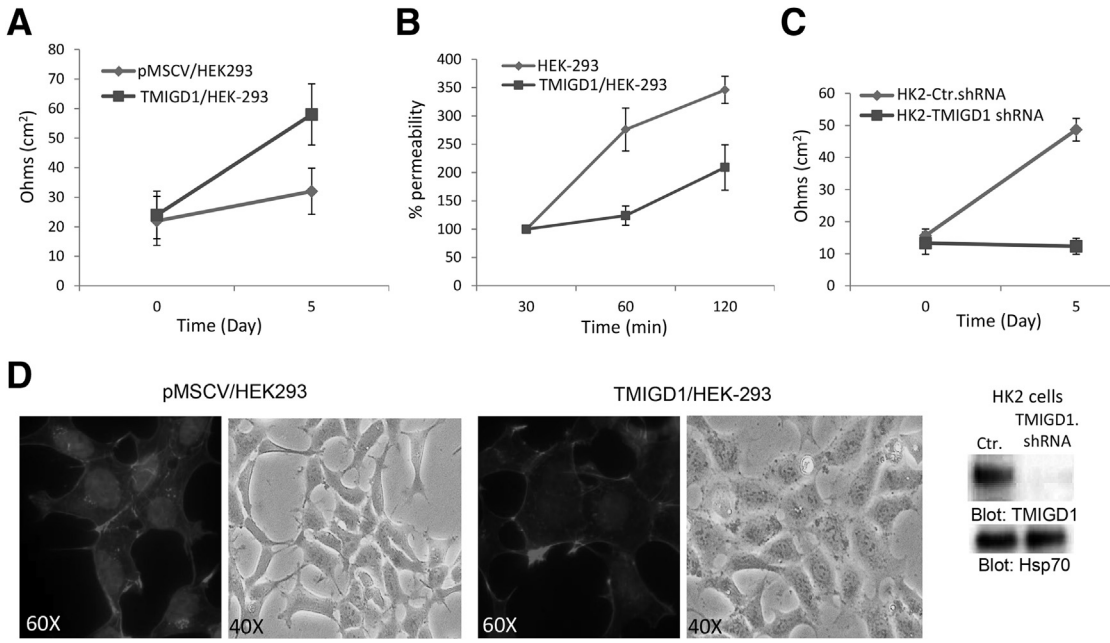

Figure 2 TMIGD1 promotes TEER of epithelial cells. **A:** Fully confluent HEK-293 cells that expressed TMIGD1 or control empty vector were seeded on the collagen-coated trans-wells, and electrical resistance was measured at day 0 and 5. **B:** Fully confluent HEK-293 cells expressing TMIGD1 or control vector were seeded on the collagen-coated trans-wells and subjected to permeability assay with fluorescently labeled dextran. Permeability was measured at 30, 60, and 120 minutes. **C:** HK2 cells that expressed control shRNA or TMIGD1 shRNA were seeded on the collagen-coated trans-wells, and electrical resistance was measured as **A**. The silencing effect of TMIGD1 shRNA on the expression of TMIGD1 in HK2 cells is shown. Whole cell lysates was blotted for TMIGD1 and loading control, Hsp70. **D:** HEK-293 cells that expressed TMIGD1 or empty vector were stained for actin with the use of phalloidin. Shown is the typical structural characteristics of HEK-293 cells that expressed TMIGD1 or control vector. Photographs were taken under light microscope. $n = 4$ Transwell per group; $n = 2$ independent experiments (**A**–**C**). Ctr, control; Hsp70, heat shock protein 70; pMSCV, empty retroviral vector; TEER, transepithelial electrical resistance; TMIGD1, transmembrane and immunoglobulin-containing 1.

Results

Identification of TMIGD1

We identified *TMIGD2* as a gene that encodes for a novel cell adhesion molecule IGPR-1. The *TMIGD2* gene is present in humans and some other mammals, but it is not present in the mouse genome.[17] Further examination of the human genome revealed the presence of a *TMIGD2*-related gene, *TMIGD1* (Ensembl gene number: ENSG00000182271; gene synonym: TMIGD, UNQ9372). TMIGD1 is located on chromosome 17 (chromosome 17: 30,316,348 to 30,334,047) with seven putative exons that encode for a protein with 262 amino acids (Figure 1A). The amino acid sequence of TMIGD1 is highly conserved in humans and mice. Human TMIGD1 has >90% sequence homology with mouse TMIGD1 (Figure 1A), and the overall amino acid sequence homology of TMIGD1 with IGPR-1 is approximately 31% (Supplemental Figure S1A). The extracellular region of TMIGD1 is predicted to contain two Ig domains and seems to form a typical Ig fold, consisting of a sandwich of two antiparallel β-sheets (Figure 1A). Phylogenetic tree analysis of *TMIGD1* revealed that *TMIGD1* gene is highly conserved among mammals and is also found in non-mammalian organisms, including *Xenopus* and *Drosophila* (Supplemental Figure S1B). One of the main differences between TMIGD1 and IGPR-1 is that TMIGD1 has a shorter cytoplasmic domain with no significant proline-rich sequences (Supplemental Figure S1A). In addition, the extracellular domain of TMIGD1 contains two putative Ig domains (Figure 1A), whereas IGPR-1 has one.[17]

We cloned TMIGD1 into a retroviral vector with a *Myc* tag at its C-terminus, and the construct was used to express TMIGD1 in HEK-293 cells. Moreover, a polyclonal anti-TMIGD1 antibody was developed to detect TMIGD1. Analysis of cell lysates from HEK-293 cells that expressed TMIGD1 found that the anti-*Myc* antibody detected a protein band with approximate molecular weight of 45 kDa in HEK-293 cells that expressed TMIGD1 (Figure 1B). Immunoblotting with the anti-TMIGD1 antibody also detected a similar protein band in cells that expressed TMIGD1 and a weaker band in the cells that expressed control vector (Figure 1B). The weaker band in HEK-293 cells that expressed empty vector likely corresponded to endogenously expressed TMIGD1 in HEK-293 cells. Preincubation of the anti-TMIGD1 antibody with a peptide used to generate anti-TMIGD1 antibody blocked the detection of both endogenous and overexpressed TMIGD1, indicating that the anti-TMIGD1 antibody specifically recognized TMIGD1 (Figure 1B). The predicted molecular weight of TMIGD1 is 29 kDa; however, both anti-*Myc* and anti-TMIGD1 antibodies detected TMIGD1 with an approximate molecular weight of 45 kDa. The higher molecular weight of TMIGD1 suggests that TMIGD1 is likely modified. We hypothesized that TMIGD1 might be *N*-glycosylated, which is common for cell surface proteins. Consistent with this possibility, treatment of cell lysate

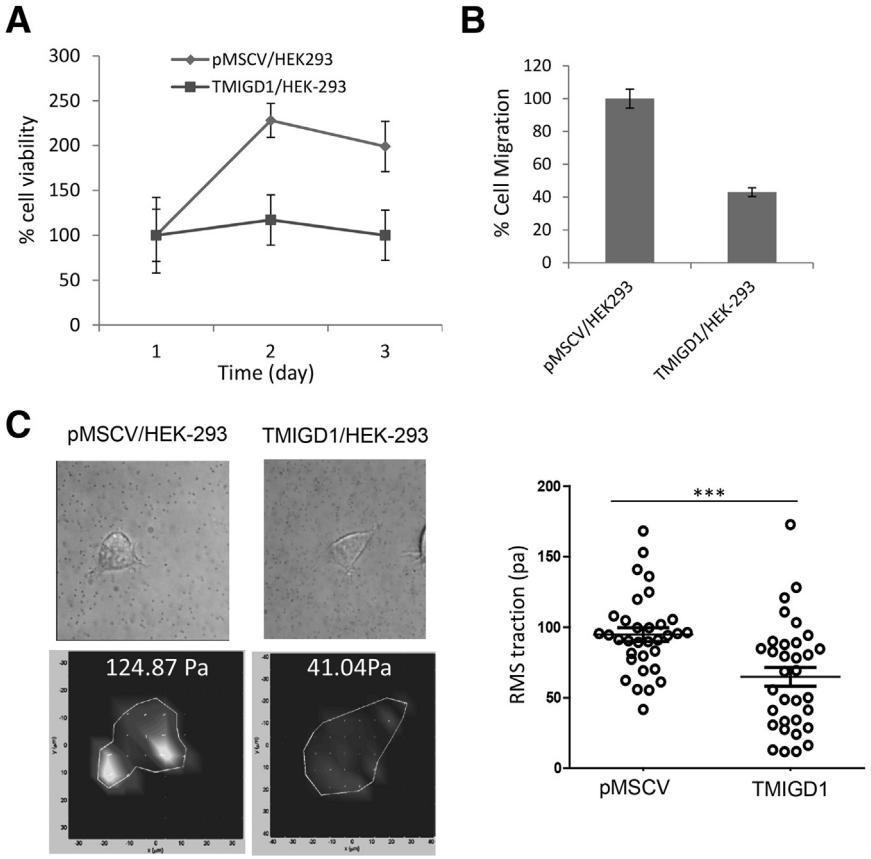

Figure 3 TMIGD1 expression in HEK-293 cells regulates cell proliferation and cell motility. **A:** HEK-293 cells that expressed TMIGD1 or empty vector were seeded on 24-well plates, and viability of cells was evaluated up to 3 days with MTT assay. **B:** HEK-293 cells expressing TMIGD1 or empty vector were seeded on Boyden chamber, and migration of cells was evaluated after 12 hours. **C:** HEK-293 cells expressing empty vector or TMIGD1 were prepared for TFM as described in *Materials and Methods*. Brightfield microscopic images and corresponding calculated traction vector maps for representative cells are shown. RMS traction calculated for each cell is indicated in the **lower right** of each traction vector map. Traction vector maps show individual calculated traction vectors at each point of the computational grid that indicate direction and magnitude and a color-coded heat map (shown here in grayscale), corresponding to traction magnitude. Individual cells were selected and imaged, and RMS traction values were calculated and shown in the graph. $n = 3$ representative experiments (**A**); $n = 4$ wells per group (**A** and **B**); $n = 2$ independent experiments (**B**). $^{***}P < 0.001$. pMSCV, empty retroviral vector; RMS, root mean square; TFM, traction force microscopy; TMIGD1, transmembrane and immunoglobulin-containing 1.

of HEK-293 cells overexpressing TMIGD1 with peptide: *N*-glycosidase F, which hydrolyzes nearly all types of *N*-glycans from glycoproteins, generated a 29-kDa protein that was recognized by anti-TMIGD1 antibody (Figure 1B). The molecular weight of endogenous TMIGD1 expressed in HK2 cells was similarly reduced by *N*-glycosidase F treatment (Supplemental Figure S2). The data indicated that a higher than expected molecular weight of TMIGD1 was due to its *N*-glycosylation.

Next, we stained HEK-293 cells that overexpressed TMIGD1 with anti-*Myc* and anti-TMIGD1 antibodies. The results found that TMIGD1 was present both at the cytoplasmic and membrane areas of HEK-293 cells (Figure 1C). Because TMIGD1 was predicted to be a cell surface protein, we performed cell surface biotinylation assay and found that TMIGD1 was localized at the cell surface of HEK-293 cells (Figure 1D).

To demonstrate expression of TMIGD1 in the mouse, we initially examined mouse kidney tissue for expression of TMIGD1. Immunohistochemical analysis of mouse tissue found that TMIGD1 was expressed in mouse kidney cells. The proximal and distal tubular epithelial cells of mouse kidney were strongly positive for TMIGD1, but TMIGD1 was low or undetectable in podocytes (Supplemental Figure S3A). In addition, cell lysates derived from human kidney tubular epithelial cells (HK2) and whole cell lysate derived from human kidney were strongly positive for TMIGD1 (Supplemental Figure S3B). Analysis of additional cell lines found that TMIGD1 was expressed in various cell lines, including breast carcinoma cell lines (BT20, HCC193), lung carcinoma (H1299), bone osteosarcoma (MG63), colon carcinoma (HCT116), and normal colon epithelial cells (NCM 460), whereas its expression was low or undetectable in colon carcinoma, HT29 cells (Supplemental Figure S3C).

Given that Ig domains are known to mediate protein–protein interactions,[27] we decided to test whether the Ig domains of TMIGD1 mediate dimerization of TMIGD1. Consistent with its known function, we found that a GST-fusion of TMIGD1 encompassing two Ig domains formed a complex with TMIGD1 (Supplemental Figure S4A), suggesting that the Ig domains of TMIGD1 acted as self-dimerization domains and could mediate its function. Because TMIGD1 was predicted to act as a cell adhesion molecule, we examined its role in mediating cell–cell interaction by subjecting them to cell aggregation assays. HEK-293 cells that expressed TMIGD1 formed large aggregates of cells compared with HEK-293 cells that expressed an empty vector (Supplemental Figure S4B). In addition, mixing of HEK-293 cells that expressed TMIGD1 with HEK-293 cells that expressed the empty vector reduced formation of large cell aggregates (Supplemental Figure S4B). The data indicated that overexpression of TMIGD1 in HEK-293 cells mediated cell–cell interaction. Aggregation assays are commonly used to assess the role of cell surface proteins, in particular, cell adhesion molecules in cell–cell interaction.

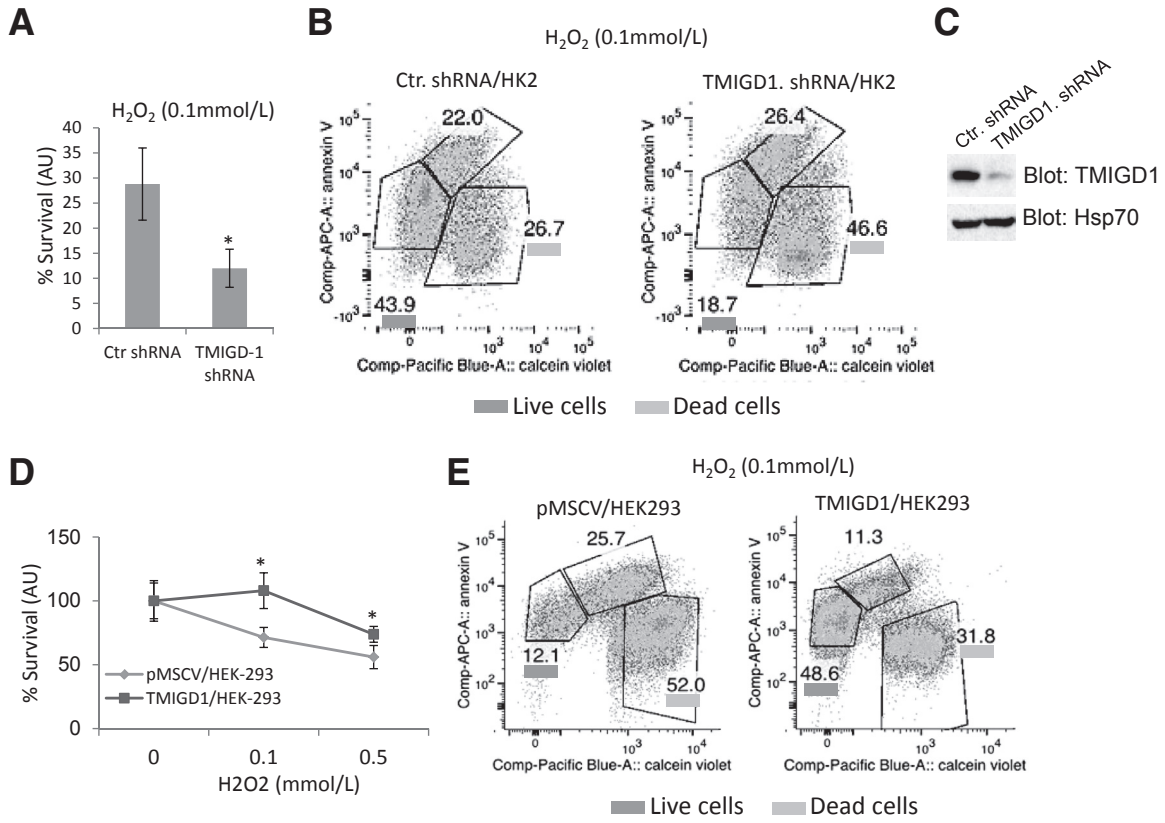

Figure 4 TMIGD1 protects kidney cells from hydrogen peroxide- and serum withdrawal-induced cell injury. **A:** HK2 cells that express control shRNA or TMIGD1 shRNA were seeded in 24-well plates in DMEM that contained 10% fetal bovine serum. After 12 hours, serum-containing medium was replaced with serum-free medium plus 0.1 mmol/L hydrogen peroxide. Cells were incubated for an additional 8 hours, and cell viability was measured by MTT assay. **B:** HK2 cells that express control shRNA or TMIGD1 shRNA also were treated with 0.1 mmol/L hydrogen peroxide for 8 hours, stained with Annexin V-FITC, and analyzed by FACS flow cytometer. **C:** Expression of TMIGD1 in HK2 cells that express control shRNA or TMIGD1 shRNA. **D:** HEK-293 cells that express TMIGD1 or control vector were seeded in 24-well plates in DMEM plus increasing concentrations of hydrogen peroxide as indicated. Cell survival was evaluated as **A**. **E:** HEK-293 cells that express control vector or TMIGD1 were treated with hydrogen peroxide as outlined in **B**, stained with annexin V-FITC, and analyzed by FACS flow cytometer. $n = 4$ wells per group (**A**); $n = 3$ independent experiments (**A**); $n = 4$ plates per group (**D**). $^*P < 0.05$ versus cells that express control shRNA or empty vector. AU, arbitrary unit; Ctr, control; DMEM, Dulbecco's modified Eagle's medium; FACS, fluorescence-activated cell sorting; FITC, fluorescein isothiocyanate; pMSCV, empty retroviral vector; TMIGD1, transmembrane and immunoglobulin-containing 1.

Overexpression of proteins involved in cell–cell interaction increased cell aggregation.[28]

TMIGD1 Regulates TEER and Permeability

Given that TMIGD1 similar to IGPR-1 acts as a cell adhesion molecule to regulate cell–cell adhesion,[17] we examined the role of TMIGD1 in TEER and cell permeability, because cell adhesion molecules are key constituents of these cellular properties.[29] Overexpression of TMIGD1 in HEK-293 cells increased TEER (Figure 2A), whereas it reduced HEK-293 cell permeability as measured with fluorescently labeled dextran (Figure 2B). Depleting TMIGD1 in primary human kidney epithelial cells (HK2) by shRNA significantly inhibited TEER (Figure 2C). Altogether, the data indicated that TMIGD1 regulated cell permeability and TEER by acting as a cell adhesion molecule.

Furthermore, expression of TMIGD1 in HEK-293 cells altered cell structural characteristics and actin stress fiber formation. In HEK-293 cells that expressed TMIGD1, actin stress fibrils were distinctively assembled at the periphery of cells, whereas in HEK-293 cells that expressed empty vector, actin fibrils were distributed central and to the periphery of cells (Figure 2D). In addition, HEK-293 cells that expressed TMIGD1 appeared to be more spread out and were larger than HEK-293 cells that expressed the empty vector (Figure 2D).

Cell–cell interaction mediated by adhesion molecules such as E-cadherin and vascular endothelial-cadherin inhibited cell proliferation and cell migration via contact inhibition.[30–33] To examine whether TMIGD1 regulates cell proliferation and migration we measured proliferation and migration of HEK-293 cells that expressed TMIGD1. Cell proliferation was measured by the reduction of the tetrazolium dye MTT by live cells. Expression of TMIGD1 in HEK-293 cells reduced the growth rate of HEK-293 cells (Figure 3A). In addition, overexpression of TMIGD1 in HEK-293 cells inhibited cell migration (Figure 3B). Given its ability to inhibit cell migration, we decided to examine the traction-generating ability of

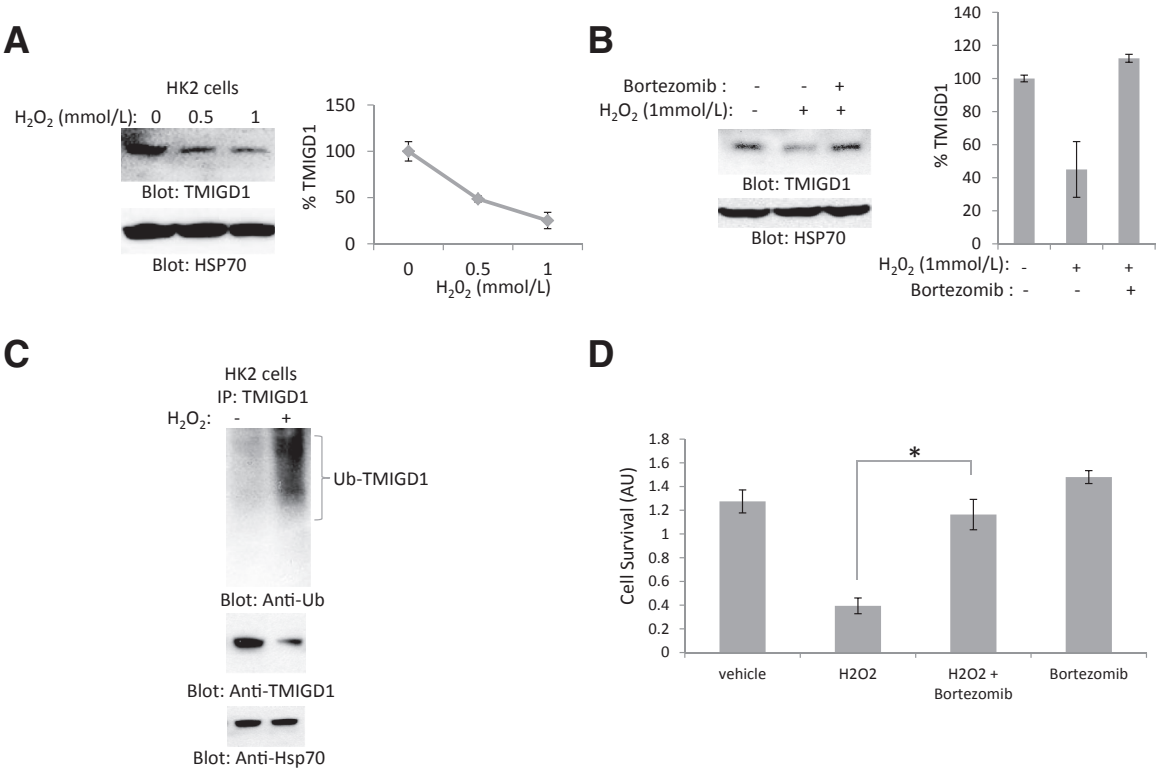

Figure 5 Oxidative stress promotes down-regulation and ubiquitination of TMIGD1. **A:** HK2 cells treated with different concentrations of hydrogen peroxide and whole cell lysates were subjected to Western blot analysis with the use of anti-TMIGD1 antibody and loading control Hsp70. **B:** HK2 cells were treated with hydrogen peroxide in the absence or presence of proteosome inhibitor bortezomib. Cells were lyzed, and whole cell lysates were blotted for TMIGD1 and loading control, Hsp70. **C:** HK2 cells were incubated in serum-free medium or medium with hydrogen peroxide, lyzed, and subjected to IP with anti-TMIGD1 antibody, followed by Western blot analysis with anti-Ub antibody. Whole cell lysates were also blotted for TMIGD1 and loading control, Hsp70. **D:** HK2 cells were seeded in 24-well plates overnight in 10% fetal bovine serum, followed by incubation of cells in serum-free medium (vehicle), serum-free medium plus hydrogen peroxide, or hydrogen peroxide plus or minus bortezomib for 8 hours. Viability of cells was evaluated with MTT assay. $n = 3$ independent experiments (**A** and **D**); $n = 2$ independent experiments (**B**). *$P < 0.05$ versus control cells treated hydrogen peroxide only. Anti-Ub, anti-ubiquitin; AU, arbitrary unit; Hsp70, heat shock protein 70; IP, immunoprecipitation; TMIGD1, transmembrane and immunoglobulin-containing 1.

HEK-293 cells that expressed TMIGD1 with the use of traction force microscopy.

Traction force microscopy revealed that HEK-293 cells that expressed TMIGD1 exhibited a significantly lower range of root mean square traction magnitudes, with a mean ± SD value of 64.87 ± 38.23 pa compared with HEK-293 cells that expressed the empty vector with a mean value of 94.71 ± 27.89 pa (Figure 3C). Taken together, the data indicated that TMIGD1 increased cell−cell adhesion and inhibited cell contractility and migration.

TMIGD1 Protects Human Kidney Epithelial Cells from Hydrogen Peroxide-Induced Cell Injury and Nutrient Deprivation

Cell adhesion plays a main role in cell injury and repair.[16] Therefore, we examined the possible function of TMIGD1 in cell injury in response to oxidative stress or nutrient deprivation. We used cell viability and Annexin V apoptosis assays to measure the protective effect of TMIGD1 to oxidative damage induced by hydrogen peroxide. Cell viability was measured by the reduction of the tetrazolium dye, MTT. Knockdown of TMIGD1 in HK2 cells considerably reduced the survival of cells (12% versus 28%) in response to hydrogen peroxide treatment (Figure 4A). Similarly, Annexin V staining found that knockdown of TMIGD1 markedly increased the susceptibility of HK2 cells to hydrogen peroxide treatment (46% versus 26% cell death) (Figure 4B). Expression of TMIGD1 in HK2 cells and the knockdown effect of TMIGD1-shRNA are shown in Figure 4C. Because knockdown of TMIGD1 increased cell death in response to hydrogen peroxide, we sought to examine whether overexpression of TMIGD1 protects cells from hydrogen peroxide-induced cell injury. Overexpression of TMIGD1 in HEK293 cells decreased survival of cells in response to hydrogen peroxide treatment as measured by cell viability (Figure 4D) and annexin V staining (Figure 4E). In addition, knockdown of TMIGD1 decreased survival of HK2 cells in nutrient-poor medium (serum free, 5 mmol/L glucose), whereas overexpression of TMIGD1 in HEK-293 cells increased survival (Supplemental Figure S5, A and B). Taken together, the data suggested that the presence of TMIGD1 increased survival of epithelial cells in response to cell injury.

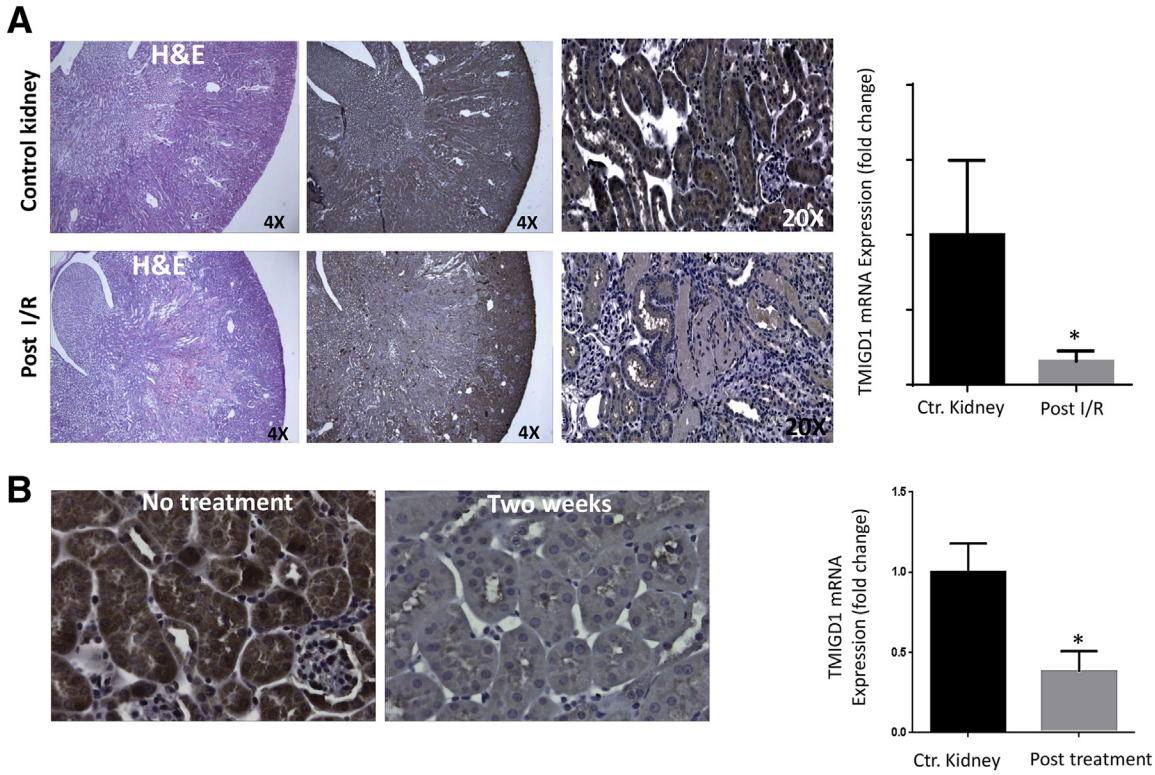

Figure 6 TMIGD1 expression is down-regulated in mouse models of kidney IR and DOCA salt uninephrectomy. **A:** The H&E staining of IR and control mouse kidney and expression of TMIGD1 in normal and IR kidneys 4 days post RI. Representative images are shown. Total mRNA was isolated from IR (4 days post RI), control mouse kidneys, and subjected to qPCR analysis. TMIGD1 mRNA expression normalized to 18S mRNA and the fold change in IR kidneys compared with control kidneys are shown. **B:** Kidney tissues from DOCA salt uninephrectomy models (two weeks post treatment) were subjected to immunohistochemistry with anti-TMIGD1 antibody, and representative images are shown. Total mRNA from two weeks post treatment was isolated from DOCA salt uninephrectomy, control mouse kidneys, and subjected to qPCR analysis. TMIGD1 mRNA expression normalized to 18S mRNA and the fold change in DOCA salt uninephrectomy kidneys compared with control are shown. Data are expressed as means ± SD. $n = 3$ control, $n = 6$ after kidney IR, $n = 3$ DOCA salt uninephrectomy. $^*P < 0.05$ versus control kidney. Ctr, control; DOCA, deoxy-corticosterone acetate; H&E, hematoxylin and eosin; IR, ischemia reperfusion; qPCR, quantitative real-time PCR; TMIGD1, transmembrane and immunoglobulin-containing 1.

Next, we examined whether expression of TMIGD1 is regulated by oxidative stress. Treatment of HK2 cells with hydrogen peroxide down-regulated TMIGD1 (Figure 5A) and treatment of cells with the proteosome inhibitor bortezomib rescued down-regulation of TMIGD1 in response to hydrogen peroxide treatment (Figure 5B). The data suggested that hydrogen peroxide targeted TMIGD1 for degradation. Because protein degradation is often mediated by ubiquitination that targets proteins for lysosomal and proteasomal degradation,[34] we examined the ubiquitination of TMIGD1 in HK2 cells in response to hydrogen peroxide. We found that treatment of HK2 cells with hydrogen peroxide induced ubiquitination of TMIGD1 (Figure 5C), indicating that hydrogen peroxide down-regulated TMIGD1 by promoting its ubiquitination.

Next, we examined whether preventing the down-regulation of TMIGD1 in response to hydrogen peroxide by bortezomib could improve the survival of cells from hydrogen peroxide-induced cell injury. The result indicated that cotreatment of HK2 cells with hydrogen peroxide and bortezomib reversed cell death caused by hydrogen peroxide (Figure 5D). Taken together, the data suggested that overexpression of TMIGD1 played a protective role and promoted cell survival under nutrient- or oxygen-deprived conditions. Furthermore, cell-damaging oxidative agents down-regulated expression and promoted ubiquitination of TMIGD1.

Expression of TMIGD1 Reduces during Kidney Cell Injury

Because TMIGD1 plays a protective role in cell injury, and oxidative stress down-regulates TMIGD1, we examined the expression status of TMIGD1 in CKD with the use of a hypertensive mouse model, and an acute renal IR model. Tubular epithelial cell injury and cell death because of apoptosis and necrosis represent the common denominator of both models.[1,35,36] On IR, tubular injury was observed in kidneys, which underwent IR after 48 hours compared with kidneys that did not receive the treatment. There was marked epithelial cell necrosis that involved most of the corticomedullary tubules (Figure 6A). Immunohistochemical analysis of normal and ischemic perfused kidney sections after ischemia found that after IR for 48 hours there was a marked increase in the staining of TMIGD1 in many epithelial cells lining the

proximal tubules compared with staining observed in the untreated samples (data not shown). However, expression of TMIGD1 was significantly reduced 4 days after IR (Figure 6A). The reduced staining of TMIGD1 was prominent mainly in the S3 segment in the outer medullary rays that corresponded to site of injury that is mainly affected, consistent with the kind of injury initiated.

In addition, we examined the expression of TMIGD1 in another mouse kidney disease model, namely in the DOCA salt-induced hypertensive mouse model of the kidney. The result indicated that expression of TMIGD1 was up-regulated after 24 hours (data not shown). However, TMIGD1 expression was substantially reduced in the morphologically normal tubules compared with tubules in the nonhypertensive mice after 2 weeks of hypertension induction (Figure 6B). The mRNA levels of TMIGD1 in post IR and DOCA salt uninephrectomy kidneys compared to controls are also shown (Figure 6, A and B). Taken together, the data indicated in mouse models of IR and CKD the expression of TMIGD1 undergoes a biphasic regulation. In the early phase of injury TMIGD1 expression was up-regulated, whereas in the late stage of injury its expression was reduced. Furthermore, these findings suggested that TMIGD1 expression was associated with survival of kidney tubules during kidney injury.

Discussion

The present work describes identification of TMIGD1 as a novel adhesion molecule expressed in kidney tubular epithelial cells, which promotes survival of kidney epithelial cells from oxidative cell injury. Kidneys are composed of hundreds of thousands of functionally independent units called nephrons, and each nephron independently controls its own permeability and solute transport capabilities by changing its adhesive characteristics on the basis of external signals. The normal function of nephrons highly depends on epithelial cell−cell adhesion and the surrounding extracellular matrix,[16,37] and adhesion molecules such as cadherins and integrins are key mediators of adhesion.[38,39] Our data indicate that TMIGD1 regulates kidney epithelial cell permeability because overexpression of TMIGD1 increased TEER and reduced permeability; reducing expression of TMIGD1 abrogated TEER. Consistent with the classical function of cell adhesion molecules, overexpression of TMIGD1 in HEK-293 cells reduced cell migration, cell proliferation, and altered the actin fibril assembly, indicating that TMIGD1 expression in epithelial cells plays a functional role in epithelial cell function.

More importantly, the data suggest that TMIGD1 is involved in ischemic renal cell injury. Reducing expression of TMIGD1 in HK2 cells significantly reduced survival of cells in response to hydrogen peroxide-induced cell injury. Similarly, overexpression of TMIGD1 in HEK-293 cells increased cell survival in response to hydrogen peroxide-mediated cell injury. Given that loss of adhesion in renal ischemia is linked to cell death,[9,40] our observation suggests an important role for TMIGD1 in renal cell injury. Curiously, another study suggests that TMIGD1 expression is down-regulated in human colon tumors,[18] indicating that perhaps in colon tumors the loss of TMIGD1 contributes to increases in tumor cell migration and proliferation, consistent with this possibility TMIGD1 overexpression in HEK-293 cells inhibited both cell proliferation and migration (Figure 3).

Underscoring the functional importance of TMIGD1 in ischemia-induced cell injury, hydrogen peroxide treatment of HK2 cells resulted in the ubiquitination and degradation of TMIGD1. Blocking the ubiquitination pathway by adding bortezomib reversed down-regulation of TMIGD1 by hydrogen peroxide. Interestingly, bortezomib treatment of HK2 cells inhibited cell death in response to hydrogen peroxide. Bortezomib treatment was studied as a possible therapeutic intervention in acute renal failure.[41] Although bortezomib is a general proteosome inhibitor, it is reasonable to speculate that agents that could up-regulate expression of TMIGD1 could potentially lead to development of a new class of drugs for treatment of renal failure. In support of a possible role of TMIGD1 in renal injury *in vivo*, TMIGD1 expression was initially up-regulated and later was substantially down-regulated in mouse models of renal injury. Although further *in vivo* studies are needed to establish a direct role for TMIGD1 in mouse renal injury, on the basis of the cell culture data it is tempting to speculate that loss of TMIGD1 may contribute in part to loss of cell adhesion and death in kidney epithelial cells.

Despite progress in renal therapy and critical care medicine, AKI still carries a high mortality rate,[1] underscoring a need for a better understating of the biology of renal cell injury and the molecules involved. Identification of TMIGD1 as a putative molecule involved in renal cell injury and further characterization of its role and the mechanisms involved should shed new light on molecular mechanism of renal cell injury.

Acknowledgments

We thank Kevin B. Chandler for comments and edits on the manuscript. The software for generating root mean square traction was kindly provided by Dr. Donald E. Ingber (Wyss Institute for Biologically Inspired Engineering, Cambridge, MA).

Supplemental Data

Supplemental material for this article can be found at *http://dx.doi.org/10.1016/j.ajpath.2015.06.006*.

References

1. Schrier RW, Wang W, Poole B, Mitra A: Acute renal failure: definitions, diagnosis, pathogenesis, and therapy. J Clin Invest 2004, 114: 5−14

2. Okusa MD, Chertow GM, Portilla D; Acute Kidney Injury Advisory Group of the American Society of Nephrology: The nexus of acute kidney injury, chronic kidney disease, and World Kidney Day 2009. Clin J Am Soc Nephrol 2009, 4:520–522
3. Xue JL, Daniels F, Star RA, Kimmel PL, Eggers PW, Molitoris BA, Himmelfarb J, Collins AJ: Incidence and mortality of acute renal failure in Medicare beneficiaries, 1992 to 2001. J Am Soc Nephrol 2006, 17:1135–1142
4. Chawla LS, Eggers PW, Star RA, Kimmel PL: Acute kidney injury and chronic kidney disease as interconnected syndromes. N Engl J Med 2014, 371:58–66
5. Grgic I, Campanholle G, Bijol V, Wang C, Sabbisetti VS, Ichimura T, Humphreys BD, Bonventre JV: Targeted proximal tubule injury triggers interstitial fibrosis and glomerulosclerosis. Kidney Int 2012, 82: 172–183
6. Sanz AB, Santamaria B, Ruiz-Ortega M, Egido J, Ortiz A: Mechanisms of renal apoptosis in health and disease. J Am Soc Nephrol 2008, 19:1634–1642
7. Versteilen AM, Di Maggio F, Leemreis JR, Groeneveld AB, Musters RJ, Sipkema P: Molecular mechanisms of acute renal failure following ischemia/reperfusion. Int J Artif Organs 2004, 27: 1019–1029
8. Myrvang H: Acute kidney injury: obesity is associated with AKI after surgery via oxidative stress. Nat Rev Nephrol 2012, 8:433
9. Sutton TA, Molitoris BA: Mechanisms of cellular injury in ischemic acute renal failure. Semin Nephrol 1998, 18:490–497
10. Molitoris BA: Actin cytoskeleton in ischemic acute renal failure. Kidney Int 2004, 66:871–883
11. Denker BM, Nigam SK: Molecular structure and assembly of the tight junction. Am J Physiol 1998, 274:F1–F9
12. Thadhani R, Pascual M, Bonventre JV: Acute renal failure. N Engl J Med 1996, 334:1448–1460
13. Heyman SN, Lieberthal W, Rogiers P, Bonventre JV: Animal models of acute tubular necrosis. Curr Opin Crit Care 2002, 8: 526–534
14. Alejandro VS, Strafuss AC: Microscopic postmortem changes in kidneys of the domestic fowl. Avian Dis 1984, 28:586–607
15. Duffield JS, Park KM, Hsiao LL, Kelley VR, Scadden DT, Ichimura T, Bonventre JV: Restoration of tubular epithelial cells during repair of the postischemic kidney occurs independently of bone marrow-derived stem cells. J Clin Invest 2005, 115: 1743–1755
16. Prozialeck WC, Edwards JR: Cell adhesion molecules in chemically-induced renal injury. Pharmacol Ther 2007, 114:74–93
17. Rahimi N, Rezazadeh K, Mahoney JE, Hartsough E, Meyer RD: Identification of IGPR-1 as a novel adhesion molecule involved in angiogenesis. Mol Biol Cell 2012, 23:1646–1656
18. Cattaneo E, Laczko E, Buffoli F, Zorzi F, Bianco MA, Menigatti M, Bartosova Z, Haider R, Helmchen B, Sabates-Bellver J, Tiwari A, Jiricny J, Marra G: Preinvasive colorectal lesion transcriptomes correlate with endoscopic morphology (polypoid vs. nonpolypoid). EMBO Mol Med 2011, 3:334–347
19. Rahimi N, Dayanir V, Lashkari K: Receptor chimeras indicate that the vascular endothelial growth factor receptor-1 (VEGFR-1) modulates mitogenic activity of VEGFR-2 in endothelial cells. J Biol Chem 2000, 275:16986–16992
20. Srinivasan S, Meyer RD, Lugo R, Rahimi N: Identification of PDCL3 as a novel chaperone protein involved in the generation of functional VEGF receptor 2. J Biol Chem 2013, 288:23171–23181
21. Matter K, Balda MS: Functional analysis of tight junctions. Methods 2003, 30:228–234
22. Meyer RD, Srinivasan S, Singh AJ, Mahoney JE, Gharahassanlou KR, Rahimi N: PEST motif serine and tyrosine phosphorylation controls vascular endothelial growth factor receptor 2 stability and down-regulation. Mol Cell Biol 2011, 31:2010–2025
23. Singh AJ, Meyer RD, Navruzbekov G, Shelke R, Duan L, Band H, Leeman SE, Rahimi N: A critical role for the E3-ligase activity of c-Cbl in VEGFR-2-mediated PLCgamma1 activation and angiogenesis. Proc Natl Acad Sci U S A 2007, 104:5413–5418
24. Meyer RD, Singh AJ, Rahimi N: The carboxyl terminus controls ligand-dependent activation of VEGFR-2 and its signaling. J Biol Chem 2004, 279:735–742
25. Butler JP, Tolic-Norrelykke IM, Fabry B, Fredberg JJ: Traction fields, moments, and strain energy that cells exert on their surroundings. Am J Physiol Cell Physiol 2002, 282:C595–C605
26. Wang Z, Gall JM, Bonegio RG, Havasi A, Hunt CR, Sherman MY, Schwartz JH, Borkan SC: Induction of heat shock protein 70 inhibits ischemic renal injury. Kidney Int 2011, 79:861–870
27. Barclay AN: Membrane proteins with immunoglobulin-like domains–a master superfamily of interaction molecules. Semin Immunol 2003, 15: 215–223
28. Balzar M, Briaire-de Bruijn IH, Rees-Bakker HA, Prins FA, Helfrich W, de Leij L, Riethmuller G, Alberti S, Warnaar SO, Fleuren GJ, Litvinov SV: Epidermal growth factor-like repeats mediate lateral and reciprocal interactions of Ep-CAM molecules in homophilic adhesions. Mol Cell Biol 2001, 21:2570–2580
29. Anderson JM, Van Itallie CM: Physiology and function of the tight junction. Cold Spring Harb Perspect Biol 2009, 1:a002584
30. Stockinger A, Eger A, Wolf J, Beug H, Foisner R: E-cadherin regulates cell growth by modulating proliferation-dependent beta-catenin transcriptional activity. J Cell Biol 2001, 154:1185–1196
31. Castilla MA, Arroyo MV, Aceituno E, Aragoncillo P, Gonzalez-Pacheco FR, Texeiro E, Bragado R, Caramelo C: Disruption of cadherin-related junctions triggers autocrine expression of vascular endothelial growth factor in bovine aortic endothelial cells: effects on cell proliferation and death resistance. Circ Res 1999, 85:1132–1138
32. Lauffenburger DA, Schaffer DV: The matrix delivers. Nat Med 1999, 5:733–734
33. Ryan PL, Foty RA, Kohn J, Steinberg MS: Tissue spreading on implantable substrates is a competitive outcome of cell-cell vs. cell-substratum adhesivity. Proc Natl Acad Sci U S A 2001, 98:4323–4327
34. Rahimi N: The ubiquitin-proteasome system meets angiogenesis. Mol Cancer Ther 2012, 11:538–548
35. Devarajan P: Update on mechanisms of ischemic acute kidney injury. J Am Soc Nephrol 2006, 17:1503–1520
36. Chen D, Coffman TM: The kidney and hypertension: lessons from mouse models. Can J Cardiol 2012, 28:305–310
37. Schneeberger EE, Lynch RD: The tight junction: a multifunctional complex. Am J Physiol Cell Physiol 2004, 286:C1213–C1228
38. Schwartz MA, Ginsberg MH: Networks and crosstalk: integrin signalling spreads. Nat Cell Biol 2002, 4:E65–E68
39. Novak A, Hsu SC, Leung-Hagesteijn C, Radeva G, Papkoff J, Montesano R, Roskelley C, Grosschedl R, Dedhar S: Cell adhesion and the integrin-linked kinase regulate the LEF-1 and beta-catenin signaling pathways. Proc Natl Acad Sci U S A 1998, 95:4374–4379
40. van Wetering S, van Buul JD, Quik S, Mul FP, Anthony EC, ten Klooster JP, Collard JG, Hordijk PL: Reactive oxygen species mediate Rac-induced loss of cell-cell adhesion in primary human endothelial cells. J Cell Sci 2002, 115:1837–1846
41. Ludwig H, Drach J, Graf H, Lang A, Meran JG: Reversal of acute renal failure by bortezomib-based chemotherapy in patients with multiple myeloma. Haematologica 2007, 92:1411–1414